

Research article

Calcineurin knockout mice show a selective loss of small spines

Hitoshi Okazaki^{a,b}, Akiko Hayashi-Takagi^{a,c,d}, Akira Nagaoka^a, Makiko Negishi^{a,b}, Hasan Ucar^{a,b}, Sho Yagishita^{a,b}, Kazuhiko Ishii^{a,b}, Taro Toyozumi^e, Kevin Fox^f, Haruo Kasai^{a,b,*}

^a Laboratory of Structural Physiology, Center for Disease Biology and Integrative Medicine, Faculty of Medicine, The University of Tokyo, Bunkyo-ku, Tokyo, Japan

^b International Research Center for Neurointelligence (WPI-IRCIN), UTIAS, The University of Tokyo, Bunkyo-ku, Tokyo, Japan

^c Laboratory of Medical Neuroscience, Institute for Molecular and Cellular Regulation, Gunma University, Maebashi-city, Gunma, Japan

^d PRESTO, Japan Science and Technology Agency, 4-1-8 Honcho, Kawaguchi, Saitama 332-0012, Japan

^e RIKEN Brain Science Institute, 2-1 Hirosawa, Wako, Saitama 351-0198, Japan

^f School of Bioscience, Cardiff University, Cardiff, UK

ARTICLE INFO

Keywords:

Dendritic spines
Synaptic plasticity
Schizophrenia
Calcineurin

ABSTRACT

Calcineurin is required for long-term depression and activity-dependent spine shrinkage, and calcineurin mutations have been identified in patients with schizophrenia. Moreover, mice with conditional knockout of calcineurin B (CNB-KO) exhibit behavioral abnormalities suggestive of schizophrenia. Changes in the dendritic spines of these mice, however, have not been investigated. We therefore examined the dendritic spines of CNB-KO mice, and observed a significant reduction in small spines and an increase in large spines in the prefrontal and visual cortices. The effect of CNB-KO on the spine sizes was relatively moderate, possibly due to the presence of spontaneous fluctuations (dynamics) in the dendritic spines themselves. Thus, CNB-KO mice showed a spine phenotype similar to those recently reported in patients with schizophrenia.

1. Introduction

Calcineurin is the only serine/threonine phosphatase controlled by Ca^{2+} /calmodulin [1], and is involved in various neuronal functions [2], including long-term depression (LTD) [3–5], spine shrinkage [6], and axonal guidance [7]. Calcineurin is a heterodimer comprising a catalytic subunit, calcineurin A (CNA), and a regulatory subunit, calcineurin B (CNB) [2]. CNB1 is an isoform of CNB and the only regulatory subunit expressed in the brain. In contrast, several different isoforms of CNA are expressed in the brain [8,9], with the *PPP3CC*-encoded γ isoform showing single-nucleotide polymorphisms in patients with schizophrenia [10–12]. CNB knockout (CNB-KO) mice exhibit certain behavioral abnormalities typically observed in schizophrenia [13], including impairments in hippocampus-dependent working memory and episodic-like memory, while contextual memory, cued fear conditioning, and spatial reference memory are all preserved [13,14].

To gain insight into the possible relationship between schizophrenic-like behavior and calcineurin dysfunction, it is valuable to study the effect of CNB-KO on spine structure *in vivo*—especially since CNB-KO should abolish activity-dependent decreases in spine size [6]. However, it is important to note that, in addition to activity-dependent

spine enlargement and shrinkage, activity-independent slow changes in spine size occur [15–21]. Such intrinsic fluctuations (dynamics) have been detected in the presence of inhibitors for NMDAR, as well as voltage-dependent Ca^{2+} and Na^{+} channels, and are known to reflect cell metabolism [15,22]. A recent study revealed that such dynamics also occur *in vivo*, and are exacerbated in autism spectrum disorders [22], further emphasizing the need to take into account activity-independent spine dynamics when assessing the influence of activity-dependent changes on spine structures.

We examined visual area V1 and frontal area 2 (Fr2), which is the rodent analogue of the dorsolateral prefrontal cortex [23], to evaluate possible differences in the distribution of spine sizes between wild-type (WT) and CNB-KO mice. We found significant differences in the distribution of spine sizes in both cortical areas. These differences, however, were relatively small, consistent with the presence of intrinsic spine dynamics.

2. Materials and methods

2.1. CNB-KO mice

Forebrain-specific CNB knockout mice, which harbor yellow

* Corresponding author at: Laboratory of Structural Physiology, Center for Disease Biology and Integrative Medicine, Faculty of Medicine, The University of Tokyo, Bunkyo-ku, Tokyo, Japan.

E-mail address: hkasai@m.u-tokyo.ac.jp (H. Kasai).

<https://doi.org/10.1016/j.neulet.2018.02.006>

Received 22 December 2017; Received in revised form 26 January 2018; Accepted 3 February 2018

Available online 07 February 2018

0304-3940/© 2018 The Author(s). Published by Elsevier B.V. This is an open access article under the CC BY-NC-ND license (<http://creativecommons.org/licenses/by-nc-nd/4.0/>).

fluorescent protein (YFP H-line in [24]) in a small subset of neurons, were generated by mating a male mouse heterozygous for floxed CNB ($CNB^{flox/wild}$ in [13]) and homozygous for the YFP allele ($YFP^{+/+}$) with a female $CNB^{flox/wild}$ mouse carrying the α -calcium-calmodulin-dependent kinase II (α CaMKII)-Cre transgene [α CaMKII-Cre $^{+/-}$]. This pairing led to the generation of $CNB^{flox/flox}$, α CaMKII-Cre $^{+/-}$, $YFP^{+/-}$ mice for the CNB-KO group and $CNB^{wild/wild}$, α CaMKII-Cre $^{+/-}$, $YFP^{+/-}$ for the littermate control (WT) group. The background strain used to generate the mutation was C57BL/6J. Mice were housed in a room with a 12-h light-dark cycle (lights on at 9:00 a.m.), with access to food and water *ad libitum*. Tail DNA was collected to identify the genotype of each animal by using polymerase chain reaction. All procedures were approved by the Animal Experiment Committee of the University of Tokyo. Procedures were carried out in accordance with the University of Tokyo Animal Care and Use Guidelines. All surgeries were performed under isoflurane anesthesia, and all efforts were made to minimize suffering.

2.2. Slice preparation

Mice were anesthetized with isoflurane, and transcardially perfused with 4% paraformaldehyde (PFA; pH 7.4); thereafter, their brains were dissected and post-fixed in 4% PFA for 12 h at room temperature. Coronal sections (150- μ m) were obtained using a vibratome (VT1000, Leica Biosystems, Germany), and brain slices were subjected to free-floating immunofluorescence staining with a slight modification to the method described in a previous study [25]. In brief, the slices were permeabilized with perm/blocking buffer (2.5% normal goat serum [v/v] in phosphate-buffered saline [PBS] with 0.1% Triton X-100 [v/v]), followed by incubation for 48 h at 4 °C with the primary antibodies against anti-green fluorescent protein (anti-GFP, D153-3, MBL, Japan). After rinsing with PBS (8 times, 5 min each), the slices were stained with the Alexa 488 goat anti-Rat IgG and mounted on slides.

2.3. Image analysis

Measurements of spine head cross-sectional areas and densities were performed using National Institutes of Health ImageJ software. Before quantifying the spine area, we binarized each imaged dendrite using the following threshold: mean value plus 4 times the standard deviation of the background intensity around the dendrite.

2.4. Statistical analysis

Distributions of spine areas were compared using the Kolmogorov–Smirnov test. Two-way analyses of variance (ANOVAs), with genotype (*i.e.*, CNB and wild-type) and cortical areas (*i.e.*, Fr2 and V1) as between-subjects factors, were performed to assess differences in spine areas and densities. ANOVAs were performed using type II sum of squares (*SS*) to adjust for unequal sample sizes, along with *post hoc* Bonferroni multiple comparison tests. We calculated eta squared η^2 , which represents the coefficient of determination for ANOVA, as

$$\eta^2 = SS_{\text{between}}/SS_{\text{total}}$$

where SS_{between} and SS_{total} represent the *SS* between groups and the overall *SS*, respectively. Within the WT and CNB-KO groups, spines were categorized into small ($< 0.3 \mu\text{m}^2$) and large sizes using Fisher's exact test.

3. Results

A confocal microscope was used to image spines in fixed slice preparations of YFP-expressing H-line mice mated with CNB-KO mice or their WT litter-mates. We investigated spines on the first branches of apical dendrites of layer 5 pyramidal neurons, where they appeared in layer 2/3 (located 200–300 μ m away from the soma), in two neocortical areas (Fr2 and V1). Mice used in this study were aged P26–32 (Fig. 1),

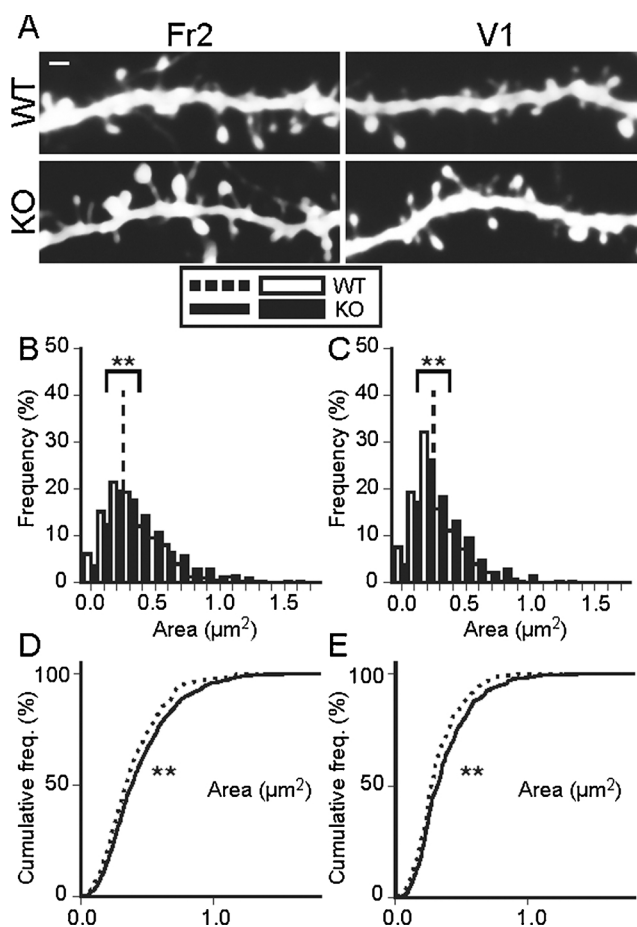


Fig. 1. Distributions of spine areas in WT and CNB-KO groups. (A) Fluorescence images of representative dendrites in the Fr2 and V1 areas of P26–32 mice. Scale bar, 1 μ m. (B, C) Distribution densities of spine areas in (B) Fr2 of P26–32 WT [574 spines, 14 dendrites, 3 mice] versus KO [709 spines, 20 dendrites, 3 mice] mice; (C), V1 of P26–32 WT [281 spines, 9 dendrites, 3 mice] versus KO [372 spines, 10 dendrites, 3 mice] mice. Vertical dashed lines indicate $0.3 \mu\text{m}^2$, and Fisher's exact tests were performed for the two populations separated by the dashed lines. n.s., not significant; $**p < 0.01$. (D, E) Cumulative distributions of spine areas in Fr2 (D) and V1 (E). The findings of Kolmogorov–Smirnov tests are presented in D and E. Statistical significances are also indicated. Error bars indicate the standard errors of the mean.

which is within the critical period for V1. In each case, spine head sizes were measured in the focal plane yielding the largest area in each case. Using this approach, we observed significant changes in the distribution of spine head sizes in both cortical areas of CNB-KO mice compared to control mice (Fig. 1B–E).

To assess whether small spines ($< 0.3 \mu\text{m}^2$) were less frequent in the cortices of CNB-KO mice than in those of WT mice, we used Fisher's exact test for WT and CNB-KO mice (Fig. 1B and C). We adopted $0.3 \mu\text{m}^2$ as the threshold for the smallest spines because morphological plasticity has been shown to decrease by at least $0.3 \mu\text{m}^2$ ($\sim 0.1 \mu\text{m}^3$ in terms of volume) when assuming that spine heads are spherical [26,27]. We found that small spines were significantly less frequent, and large spines more frequent, in CNB-KOs than in WT mice for both Fr2 and V1 cortices.

Previous studies have reported that mean spine head area varies by cortical region and that, in the mouse, spine heads are largest in the motor cortex [28]. Similarly, in this study, we found that mean spine head area varied between Fr2 and V1 in WT mice (Fig. 2), with spines in Fr2 being significantly larger than those in V1 (Fig. 2). On the other hand, mean spine areas in CNB-KO mice were larger in both Fr2 and V1 than in WT mice (Fig. 2). A two-way ANOVA showed a significant effect

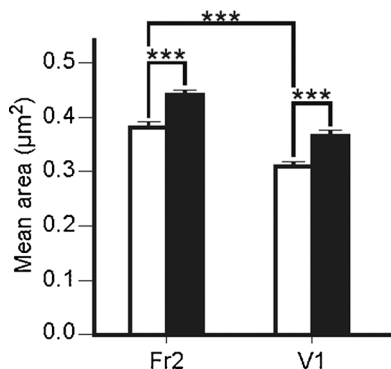


Fig. 2. Mean spine areas in WT and CNB-KO groups.

Mean spine areas were significantly different according to genotypes and cortical areas, as determined by two-way analyses of variance. All spine area p values were adjusted by the Bonferroni method for multiple comparisons; *** $p < 0.001$. Error bars indicate the standard errors of the mean.

of genotype across the two cortical areas (15–18%; ANOVA: $p < 0.001$, $\eta^2 = 0.014$) but no significant interaction between genotype and cortical area ($p > 0.05$). Interestingly, the differences between WT and CNB-KO mice did not appear to be larger than the difference between the two cortical areas in WT or CNB-KO mice (21–24%; ANOVA: $p < 0.001$, $\eta^2 = 0.021$). Moreover, overall, the difference in spine head size due to CNB knockout was rather small.

Since spine density is often affected in patients with schizophrenia [29–31], we also examined the number of spines in WT and CNB-KO mice. However, no significant difference in spine density was found between phenotypes for Fr2 nor V1; spine density (spine number/µm) in Fr2 was 1.45 ± 0.08 (mean \pm standard error, $n = 16$) and 1.63 ± 0.12 ($n = 8$) for WT and KO mice, respectively ($p = 0.22$), while the spine density in V1 was 1.25 ± 0.07 ($n = 14$) and 1.60 ± 0.18 ($n = 6$) for WT and KO mice, respectively ($p = 0.06$).

4. Discussion

Consistent with our hypothesis, we found a reduction in small spines in CNB-KO mice, suggesting that the prevention of spine shrinkage in these animals allows small spines to be readily enlarged. Previous studies have shown that CNB-KO mice exhibit schizophrenia-like behaviors, such as weak spatial working memory and normal spatial reference memory [14]. The formation of working memory requires rapid synaptic changes and likely involves small spines which undergo more pronounced enlargement [15,26,27,32,33]. In CNB-KO mice, working memory deficits may reflect a reduction in the number of small spines that are available for potentiation and enlargement. Recently, a systematic postmortem study of human patients with schizophrenia reported a specific loss of small spines in the neocortex [31,34]—consistent with our current findings in CNB-KO mice.

The differences between CNB-KO and WT mice observed in the current study were relatively moderate (Fig. 1F). In contrast, activity-dependent spine shrinkage is typically severe [6], and predicts the marked enlargement of spines. This discrepancy may be explained by intrinsic dynamics in spine volume which, unlike activity-dependent plasticity, occur continuously over long periods of time and are the major factor determining spine size distributions [15,35]. Due to these intrinsic dynamics, large spines can shrink back to small spines, and CNB-KO may only have a more moderate influence on spine size distribution than the differences between cortical regions.

In conclusion, our current findings of a moderate reduction in small spine densities in CNB-KO mice are akin to observations made in patients with schizophrenia. Further, we hypothesize that CNB-KO-induced reductions were moderate because of the presence of spontaneous dynamics in dendritic spine sizes.

Acknowledgements

We thank T. Miyakawa for providing the CNB-KO mice and for the helpful discussions. We also thank Ogasawara, H. Ohno, Tajiri, M. and M. Nakamura for their technical assistance. This work was supported by Grants-in-Aid for Scientific Research (S) (No. 26221001 to HK), (B) (No. 26293260 to AH-T), Young Scientists (B)(15K18333 to SY) and Scientific Research on Innovative Areas (16H06396 to SY) from JSPS, and CREST (JPMJCR1652 to HK) from JST, and the SICP, Brain/MIND, Strategic Research Program for Brain Sciences projects (SRPBS, 17dm0107120h0002) from AMED (to HK), and World Premier International Research Center Initiative (WPI) from MEXT (to HK). KF was supported by an MRC/JST International collaborative award (MR/M501670/1). TT was supported by Brain/MINDS from AMED and RIKEN Brain Science Institute.

Appendix A. Supplementary data

Supplementary data associated with this article can be found, in the online version, at <https://doi.org/10.1016/j.neulet.2018.02.006>.

References

- [1] C.B. Klee, H. Ren, X. Wang, Regulation of the calmodulin-stimulated protein phosphatase, calcineurin, *J. Biol. Chem.* 273 (1998) 13367–13370.
- [2] F. Rusnak, P. Mertz, Calcineurin: form and function, *Physiol. Rev.* 80 (2000) 1483–1521.
- [3] R.M. Mulkey, S. Endo, S. Shenolikar, R.C. Malenka, Involvement of a calcineurin/inhibitor-1 phosphatase cascade in hippocampal long-term depression, *Nature* 369 (1994) 486–488.
- [4] H. Zeng, S. Chattarji, M. Barbarosie, L. Rondi-Reig, B.D. Philpot, T. Miyakawa, M.F. Bear, S. Tonegawa, Forebrain-specific calcineurin knockout selectively impairs bidirectional synaptic plasticity and working/episodic-like memory, *Cell* 107 (2001) 617–629.
- [5] Q. Zhou, K.J. Homma, M.M. Poo, Shrinkage of dendritic spines associated with long-term depression of hippocampal synapses, *Neuron* 44 (2004) 749–757.
- [6] T. Hayama, J. Noguchi, S. Watanabe, N. Takahashi, A. Hayashi-Takagi, G.C. Ellis-Davies, M. Matsuzaki, H. Kasai, GABA promotes the competitive selection of dendritic spines by controlling local Ca²⁺ signaling, *Nat. Neurosci.* 16 (2013) 1409–1416.
- [7] Z. Wen, C. Guirland, G.L. Ming, J.Q. Zheng, A CaMKII/calcineurin switch controls the direction of Ca(2+)-dependent growth cone guidance, *Neuron* 43 (2004) 835–846.
- [8] T. Takaishi, N. Saito, T. Kuno, C. Tanaka, Differential distribution of the mRNA encoding two isoforms of the catalytic subunit of calcineurin in the rat brain, *Biochem. Biophys. Res. Commun.* 174 (1991) 393–398.
- [9] T. Kuno, H. Mukai, A. Ito, C.D. Chang, K. Kishima, N. Saito, C. Tanaka, Distinct cellular expression of calcineurin A alpha and A beta in rat brain, *J. Neurochem.* 58 (1992) 1643–1651.
- [10] D.J. Gerber, D. Hall, T. Miyakawa, S. Demars, J.A. Gogos, M. Karayiorgou, S. Tonegawa, Evidence for association of schizophrenia with genetic variation in the Sp21.3 gene, PPP3CC, encoding the calcineurin gamma subunit, *Proc. Natl. Acad. Sci. U. S. A.* 100 (2003) 8993–8998.
- [11] Y.L. Liu, C.S. Fann, C.M. Liu, C.C. Chang, W.C. Yang, S.I. Hung, S.L. Yu, T.J. Hwang, M.H. Hsieh, C.C. Liu, M.M. Tsuang, J.Y. Wu, Y.S. Jou, S.V. Faraone, M.T. Tsuang, W.J. Chen, H.G. Hwu, More evidence supports the association of PPP3CC with schizophrenia, *Mol. Psychiatry* 12 (2007) 966–974.
- [12] K. Yamada, D.J. Gerber, Y. Iwayama, T. Ohnishi, H. Ohba, T. Toyota, J. Aruga, Y. Minabe, S. Tonegawa, T. Yoshikawa, Genetic analysis of the calcineurin pathway identifies members of the EGR gene family, specifically EGR3, as potential susceptibility candidates in schizophrenia, *Proc. Natl. Acad. Sci. U. S. A.* 104 (2007) 2815–2820.
- [13] T. Miyakawa, L.M. Leiter, D.J. Gerber, R.R. Gainetdinov, T.D. Sotnikova, H. Zeng, M.G. Caron, S. Tonegawa, Conditional calcineurin knockout mice exhibit multiple abnormal behaviors related to schizophrenia, *Proc. Natl. Acad. Sci. U. S. A.* 100 (2003) 8987–8992.
- [14] H. Zeng, S. Chattarji, M. Barbarosie, L. Rondi-Reig, B.D. Philpot, T. Miyakawa, M.F. Bear, S. Tonegawa, Forebrain-specific calcineurin knockout selectively impairs bidirectional synaptic plasticity and working/episodic-like memory, *Cell* 107 (2001) 617–629.
- [15] N. Yasumatsu, M. Matsuzaki, T. Miyazaki, J. Noguchi, H. Kasai, Principles of long-term dynamics of dendritic spines, *J. Neurosci.* 28 (2008) 13592–13608.
- [16] A. Statman, M. Kaufman, A. Minerbi, N.E. Ziv, N. Brenner, Synaptic size dynamics as an effectively stochastic process, *PLoS Comput. Biol.* 10 (2014) e1003846.
- [17] A. Fisher-Lavie, N.E. Ziv, Matching dynamics of presynaptic and postsynaptic scaffolds, *J. Neurosci.* 33 (2013) 13094–13100.
- [18] Y. Loewenstein, A. Kuras, S. Rumpel, Multiplicative dynamics underlie the emergence of the log-normal distribution of spine sizes in the neocortex in vivo, *J. Neurosci.* 31 (2011) 9481–9488.

- [19] R. Dvorkin, N.E. Ziv, Relative contributions of specific activity histories and spontaneous processes to size remodeling of glutamatergic synapses, *PLoS Biol.* 14 (2016) e1002572.
- [20] G. Mongillo, S. Rumpel, Y. Loewenstein, Intrinsic volatility of synaptic connections — a challenge to the synaptic trace theory of memory, *Curr. Opin. Neurobiol.* 46 (2017) 7–13.
- [21] A.R. Chambers, S. Rumpel, A stable brain from unstable components: emerging concepts and implications for neural computation, *Neuroscience* 357 (2017) 172–184.
- [22] A. Nagaoka, H. Takehara, A. Hayashi-Takagi, J. Noguchi, K. Ishii, F. Shirai, S. Yagishita, T. Akagi, T. Ichiki, H. Kasai, Abnormal intrinsic dynamics of dendritic spines in a fragile X syndrome mouse model in vivo, *Sci. Rep.* 6 (2016) 26651.
- [23] H.B.M. Uylings, H.J. Groenewegen, B. Kolb, Do rats have a prefrontal cortex? *Behav. Brain Res.* 146 (2003) 3–17.
- [24] G. Feng, R.H. Mellor, M. Bernstein, C. Keller-Peck, Q.T. Nguyen, M. Wallace, J.M. Nerbonne, J.W. Lichtman, J.R. Sanes, Imaging neuronal subsets in transgenic mice expressing multiple spectral variants of GFP, *Neuron* 28 (2000) 41–51.
- [25] A. Hayashi-Takagi, S. Yagishita, M. Nakamura, F. Shirai, Y.I. Wu, A.L. Loshbaugh, B. Kuhlman, K.M. Hahn, H. Kasai, Labelling and optical erasure of synaptic memory traces in the motor cortex, *Nature* 525 (2015) 333–338.
- [26] J. Tanaka, Y. Horiike, M. Matsuzaki, T. Miyazaki, G.C. Ellis-Davies, H. Kasai, Protein synthesis and neurotrophin-dependent structural plasticity of single dendritic spines, *Science* 319 (2008) 1683–1687.
- [27] M. Matsuzaki, N. Honkura, G.C. Ellis-Davies, H. Kasai, Structural basis of long-term potentiation in single dendritic spines, *Nature* 429 (2004) 761–766.
- [28] I. Ballesteros-Yanez, R. Benavides-Piccione, G.N. Elston, R. Yuste, J. DeFelipe, Density and morphology of dendritic spines in mouse neocortex, *Neuroscience* 138 (2006) 403–409.
- [29] L.J. Garey, W.Y. Ong, T.S. Patel, M. Kanani, A. Davis, A.M. Mortimer, T.R. Barnes, S.R. Hirsch, Reduced dendritic spine density on cerebral cortical pyramidal neurons in schizophrenia, *J. Neurol. Neurosurg. Psychiatry* 65 (1998) 446–453.
- [30] J.R. Glausier, D.A. Lewis, Dendritic spine pathology in schizophrenia, *Neuroscience* 251 (2013) 90–107.
- [31] J.T. Coyle, Cortical pyramidal neurons show a selective loss of new synapses in chronic schizophrenia, *Am. J. Psychiatry* 174 (2017) 510–511.
- [32] H. Kasai, M. Fukuda, S. Watanabe, A. Hayashi-Takagi, J. Noguchi, Structural dynamics of dendritic spines in memory and cognition, *Trends Neurosci.* 33 (2010) 121–129.
- [33] J. Noguchi, M. Matsuzaki, G.C. Ellis-Davies, H. Kasai, Spine-neck geometry determines NMDA receptor-dependent Ca²⁺ signaling in dendrites, *Neuron* 46 (2005) 609–622.
- [34] M.L. MacDonald, J. Alhassan, J.T. Newman, M. Richard, H. Gu, R.M. Kelly, A.R. Sampson, K.N. Fish, P. Penzes, Z.P. Wills, D.A. Lewis, R.A. Sweet, Selective loss of smaller spines in schizophrenia, *Am. J. Psychiatry* 174 (2017) 586–594 [appi.ajp.2017.16070814](https://doi.org/10.1176/appi.ajp.2017.16070814).
- [35] Y. Loewenstein, U. Yanover, S. Rumpel, Predicting the dynamics of network connectivity in the neocortex, *J. Neurosci.* 35 (2015) 12535–12544.